

# First-principles study of phase stability of Ti<sub>2</sub>N under pressure

V. I. Ivashchenko,<sup>1</sup> P. E. A. Turchi,<sup>2</sup> V. I. Shevchenko,<sup>1</sup> and E. I. Olifan<sup>1</sup>

<sup>1</sup>*Institute of Problems of Material Science, NAS of Ukraine, Krzhynozhansky strasse 3, 03142 Kyiv, Ukraine*

<sup>2</sup>*Lawrence Livermore National Laboratory (L-352), P. O. Box 808, Livermore, California 94551, USA*

(Received 12 April 2012; revised manuscript received 3 July 2012; published 16 August 2012)

A first-principles study of phase stability of various phases of Ti<sub>2</sub>N under normal conditions and as a function of pressure was carried out. Among the  $\epsilon$  and  $\delta'$  phases of Ti<sub>2</sub>N that are observed experimentally,  $\epsilon$ -Ti<sub>2</sub>N is the most stable. The  $\delta'$  phase can only exist at high temperature due to the soft acoustic modes at the  $X$  point. The origin of the tetragonal structure of both the  $\epsilon$  and  $\delta'$  phases is supposed to be caused by the tetragonal local lattice distortion around a nitrogen vacancy. Based on the results of the total-energy and phonon-spectrum calculations at zero temperature, the following sequence of phase transformation in Ti<sub>2</sub>N under pressure is predicted:  $\epsilon$ -Ti<sub>2</sub>N (space group  $P4/mnm$ ),  $P = 77.5$  GPa  $\rightarrow$  Au<sub>2</sub>Te type (space group  $C2/m$ ),  $P = 86.7$  GPa  $\rightarrow$  Al<sub>2</sub>Cu type (space group  $I4/mcm$ ). The present study shows that, to correctly predict relative phase stability, the peculiarities of the phonon spectra of the materials under investigation have to be properly accounted for.

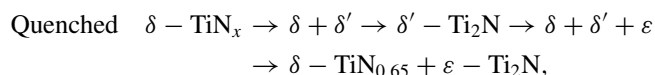
DOI: 10.1103/PhysRevB.86.064109

PACS number(s): 62.50.-p, 63.20.dk, 64.60.Ej, 71.15.Nc

## I. INTRODUCTION

Titanium nitrides TiN<sub>*x*</sub> form a class of materials with the NaCl-type crystal structure ( $B1$ ) in the homogeneity range  $0.38 < x < 1.15$ , and exhibit extremely high melting points, hardness, and metallic conductivity.<sup>1,2</sup> These materials are widely used as main layers in ultrahard nano-composite coatings.<sup>3</sup> In transition metal compounds (TMC), nonmetal vacancies are not randomly distributed, but instead display long- or short-range order. In addition, vacancies induce small local distortions of the lattice.<sup>2</sup>

In the present study, we focus on the titanium nitride Ti<sub>2</sub>N, or TiN<sub>*x*</sub> with the composition  $x = 0.5$ . At low nitrogen content ( $0.38 < x < 0.61$ ), TiN<sub>*x*</sub> annealed below 1073 K exhibits a  $\delta'$ -Ti<sub>2</sub>N (TiN<sub>*x*</sub>,  $x = 0.5$ ) superstructure (space group  $I4_1/amd$ ).<sup>4</sup> This superstructure is metastable since, at 1023 K, the following phase-transformation sequence has been directly observed by neutron diffraction:<sup>5</sup>



where  $\delta$  is a distorted  $B1$ -TiN<sub>*x*</sub> structure, and  $\epsilon$ -Ti<sub>2</sub>N (TiN<sub>*x*</sub>,  $x = 0.5$ ) is a stable phase with the tetragonal antirutile structure (space group  $P4_2/mnm$ ).<sup>6</sup>

Recently, it was shown that the homogeneity ranges of the  $\epsilon$ - and  $\delta'$ -phases of TiN<sub>*x*</sub> are  $0.38 \leq x \leq 0.42$ , and  $0.45 \leq x \leq 0.5$ , respectively.<sup>7</sup> This finding is not consistent with the results of the previous structural investigations,<sup>4-6</sup> in which the authors found that both the  $\epsilon$  and  $\delta'$  phases of TiN<sub>*x*</sub> could exist in the range  $0.38 < x < 0.61$ . Also, experimental investigations disagree with regard to the stability of the  $\epsilon$  and  $\delta'$  phases. In particular, according to previous observations,<sup>8-10</sup>  $\delta'$ -Ti<sub>2</sub>N is a metastable phase that exists in a narrow temperature range 900–1180 K, whereas in other instances this phase was found to be stable below 900–1000 K (Refs. 6 and 11–13).

Band-structure and total-energy calculations of both phases of Ti<sub>2</sub>N were carried out by Eibler using the full-potential linearized augmented plane-wave (FLAPW) method.<sup>14,15</sup> However, to our knowledge, electronic and phonon structures and

the phase stability of Ti<sub>2</sub>N under pressure were not investigated at all.

In the present work, we plan to fill this gap by studying the properties of Ti<sub>2</sub>N. We report on the results of first-principles investigations of phase stability and the electronic and phonon structures of Ti<sub>2</sub>N under pressure. The relative phase stability of the  $\epsilon$  and  $\delta'$  phases, as well as of other phases of Ti<sub>2</sub>N under pressure was analyzed by taking into account the results of both total energies and phonon spectra.

The paper is organized as follows. In Sec. II we present our theoretical framework and the computational details. Section III contains the results of our calculations together with comments. Finally, Sec. IV contains the main conclusions.

## II. COMPUTATIONAL ASPECTS

A first-principles pseudopotential procedure was employed to investigate the cubic, tetragonal, hexagonal, monoclinic, orthorhombic, and triclinic structures of Ti<sub>2</sub>N. Scalar-relativistic band-structure calculations within the density functional theory (DFT) were carried out for different structures of Ti<sub>2</sub>N. To investigate the lattice relaxation around a nitrogen vacancy, the initial 64-atom ( $2 \times 2 \times 2$ ) supercell of  $B1$ -type TiN was constructed from the basic eight-atom cubic cell, and a single vacancy was placed in the center of the supercell. Also, we calculated the atomic configurations of the two clusters NTi<sub>14</sub>N<sub>18</sub> and Ti<sub>14</sub>N<sub>18</sub>. These structures were considered as periodic cubic structures with a large lattice parameter of 17 Å, which guarantees that the atoms interact only inside the same unit cell.

The “QUANTUM-ESPRESSO” first-principles code<sup>16</sup> was used to perform the pseudopotential calculations with Vanderbilt ultrasoft pseudopotentials to describe the electron-ion interaction.<sup>17</sup> In the Vanderbilt approach,<sup>17</sup> the orbitals are allowed to be as soft as possible in the core region so that their plane-wave expansion converged rapidly. For titanium, the semicore states were treated as valence states. Plane waves up to a kinetic energy cutoff of 30 Ry were included in the basis set. The exchange-correlation potential was treated in the framework of the generalized gradient approximation

(GGA) of Perdew-Burke-Ernzerhof (PBE).<sup>18</sup> Brillouin-zone integrations have been performed using sets of special points corresponding to the (8 8 8) (the three-atomic cells) and (4 4 4) (the 6–12-atomic cells) Monkhorst-Park meshes.<sup>19</sup> For the large supercells, we considered the (2 2 2) mesh that, although it generates a minimum number of  $k$  points, provides an acceptable accuracy. Each eigenvalue was convoluted with a Gaussian with width  $\sigma = 0.02$  Ry (0.272 eV). All structures were optimized by simultaneously relaxing the atomic basis vectors and the atomic positions inside the unit cells using the Broyden-Fletcher-Goldfarb-Shanno (BFGS) algorithm.<sup>20</sup> The relaxation of the atomic coordinates and of the unit cell was considered to be complete when the atomic forces were less than 1.0 mRy/Bohr (25.7 meV/Å), the stresses were smaller than 0.025 GPa, and the total energy during the structural optimization iterative process was varying by less than 0.1 mRy (1.36 meV). The crystalline and energetic parameters of the structures of Ti<sub>2</sub>N under investigation obtained after structural optimization are summarized in Table I. The electronic densities of states (DOS) and the Fermi surfaces were calculated using the (12 12 12) mesh.

The above-described pseudopotential procedure was used to study the phonon spectra of tetragonal, hexagonal, and triclinic Ti<sub>2</sub>N in the framework of the density-functional perturbation theory (DFPT) described in Refs. 16 and 21. The first-principles DFPT calculations were carried out for the (4 4 4)  $q$  mesh, and then the phonon densities of states (PHDOS) were computed using the (12 12 12)  $q$  mesh by interpolating the computed phonon dispersion curves. Both the DOS and PHDOS were calculated with the tetra-

hedron method implemented in the “QUANTUM-ESPRESSO” code.<sup>16</sup>

To verify an acceptability of the chosen conditions of the calculations we estimate the heat of formation of TiN and  $\varepsilon$ -Ti<sub>2</sub>N,  $H^f$ , using the expression  $H^f = E_{\text{tot}} - \sum n_i E_i$ , where  $E_{\text{tot}}$  is the total energy of the bulk compound with  $n_i$  atoms of all involved elements  $i$  (Ti and N) and  $E_i$  is the total energy of the bulk hexagonal close-packed Ti (space group  $P6_3/mmc$ , No. 194), and half of the energy of the N<sub>2</sub> molecule, respectively. The total energy and equilibrium bond length of the N<sub>2</sub> molecule were computed using the extended two-atom cubic cell. The bond length of the N<sub>2</sub> molecule was in agreement with the experimental value (1.098 Å) within 1%. The computed values of  $H^f$  for TiN and  $\varepsilon$ -Ti<sub>2</sub>N are  $-3.46$  and  $-3.98$ , respectively, which are in good agreement with the corresponding experimental values of 3.46 (Ref. 22) and 4.12 (Ref. 23) and theoretical values of 3.34 and 3.86 (Ref. 15), respectively (in units eV/formula unit). It follows that  $\varepsilon$ -Ti<sub>2</sub>N is stable over TiN + Ti since the heat of formation of this reaction is  $-0.52$  eV/formula unit.

### III. RESULTS AND DISCUSSION

#### A. Ti<sub>2</sub>N structures at equilibrium

To predict possible stable structures of Ti<sub>2</sub>N, at first we calculated the total energy of  $\delta'$ -Ti<sub>2</sub>N and  $\varepsilon$ -Ti<sub>2</sub>N, as well of different phases of Ti<sub>2</sub>N that were identified for other TMC (V<sub>2</sub>N, Nb<sub>2</sub>N, Ti<sub>2</sub>C, V<sub>2</sub>C, W<sub>2</sub>C, Mo<sub>2</sub>C, Co<sub>2</sub>Si, etc.)<sup>1,2</sup> at equilibrium. The unit cells of the most stable phases of Ti<sub>2</sub>N are shown in Fig. 1. One can see from Table I that, at

TABLE I. Symmetry, structural parameters, and total energy ( $E_T$ ) (relative to  $E_T$  of  $\varepsilon$ -Ti<sub>2</sub>N) of the calculated phases of Ti<sub>2</sub>N.

Phase	Space group	No	N <sub>a</sub>	$a$ (Å)	$b$ (Å)	$c$ (Å)	$V$ (Å <sup>3</sup> /atom)	$\Delta E_T$ (eV/atom)
$\varepsilon$ -Ti <sub>2</sub> N	$P4_2/mnm$	136	6	4.928	4.928	3.021	12.228	0.000
	Tetragonal			(4.945) <sup>a</sup>	(4.945) <sup>a</sup>	(3.034) <sup>a</sup>	(12.365) <sup>a</sup>	
$\delta'$ -Ti <sub>2</sub> N	$I4_1/amd$	141	6	4.132	4.132	8.806	12.523	0.011
	Tetragonal			(4.149) <sup>b</sup>	(4.149) <sup>b</sup>	(8.786) <sup>b</sup>	(12.604) <sup>b</sup>	
Cd <sub>2</sub> I(anti-CdI <sub>2</sub> )	$P-3m1$ Hexagonal	164	3	2.983	2.983	4.760	12.225	0.017
Au <sub>2</sub> Te <sup>c</sup>	$C2/m$	12	6	5.136	3.002	4.761		
	Monoclinic			90°	92.27°	90°	~12.225	0.017
(anti-AuTe <sub>2</sub> )	$P1$	1	3	2.974	2.974	4.761		
$\varepsilon$ -Fe <sub>2</sub> N	Triclinic			88.04°	91.96°	119.39°		
	$P-31m$ Hexagonal	162	9	5.123	5.123	4.759	12.024	0.051
Ti <sub>2</sub> C <sup>c</sup>	$Fd-3m$ Cubic	227	48	8.389	8.389	8.389		
	$R-3m$	166	12	5.932	5.932	5.932		0.073
	Rhombohedral			60°	60°	60°	12.298	
Co <sub>2</sub> Si	$Pnma$ Orthorhombic	62	12	4.181	4.151	8.2998	12.003	0.196
Al <sub>2</sub> Cu	$I4/mcm$ Tetragonal	140	6	5.167	5.167	4.978	11.160	0.533
Ti <sub>2</sub> C	$R-3m$	166	3	3.454	3.454	3.454	11.624	0.674
	Rhombohedral			69.42°	69.42°	69.42°		
Fe <sub>2</sub> P	$P-62m$ Hexagonal	189	9	6.048	6.048	3.120	10.978	0.712
$\xi$ -Fe <sub>2</sub> N	$Pbcn$ Orthorhombic	60	12	5.168	6.512	4.211	11.807	0.742
Cu <sub>2</sub> Sb	$P4/nmm$ Tetragonal	129	6	3.248	3.248	6.262	11.010	0.796
Ge <sub>2</sub> Ta	$P6_222$ Hexagonal	180	9	4.698	4.698	5.362	11.386	1.173
$\gamma$ -W <sub>2</sub> C	$P6_3/mmc$ Hexagonal	194	6	4.153	4.153	4.845	9.881	1.307

<sup>a</sup>X-ray diffraction experiments (Ref. 6).

<sup>b</sup>Neutron diffraction experiments (Ref. 12).

<sup>c</sup>These phases can be represented by two structures that have the same total energies and cell volumes.

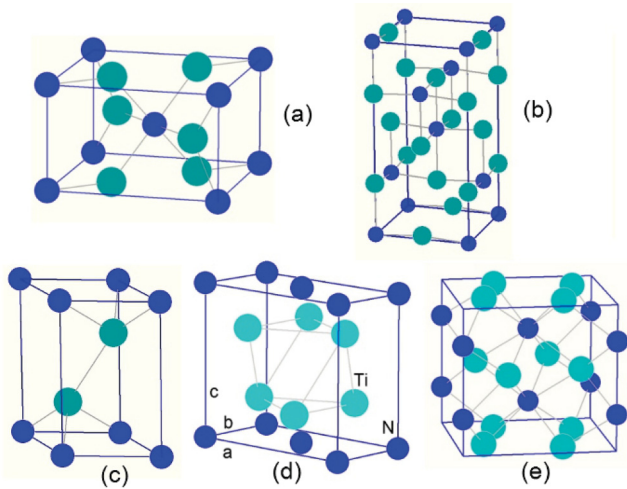


FIG. 1. (Color online) Primitive unit cells of (a)  $\epsilon$ - $\text{Ti}_2\text{N}$ , (b)  $\delta'$ - $\text{Ti}_2\text{N}$ , (c) Cd<sub>2</sub>I-type  $\text{Ti}_2\text{N}$ , (d) Au<sub>2</sub>Te-type  $\text{Ti}_2\text{N}$ , and (e) Al<sub>2</sub>Cu-type  $\text{Ti}_2\text{N}$ .

zero pressure,  $\epsilon$ - $\text{Ti}_2\text{N}$  is the most stable phase in agreement with the experiment<sup>6</sup> and previous total-energy calculations.<sup>15</sup> The  $\delta'$ - $\text{Ti}_2\text{N}$  phase has a slightly higher total energy and cell volume than those for  $\epsilon$ - $\text{Ti}_2\text{N}$ . The total energy difference equal to 3.068 kJ/mol confirms the value determined by Eibler (3.3 kJ/mol) (Ref. 15). The computed and experimental structural parameters, lattice parameters, and cell volumes, shown in Table I, agree very well.

The electronic band structure and densities of states (DOS) of the  $\epsilon$  and  $\delta'$ - $\text{Ti}_2\text{N}$  phases are shown in Fig. 2. The lowest bands are associated with the 2s states of N. The next band around  $-5$  eV originates from N 2p and Ti 3d states. Finally, the broad Ti d band with a small admixture of N 2p states is located above the minimum of the DOS (around  $-3.5$  eV). One can see that the electronic spectra of both phases are similar. The Fermi level ( $E_F$ ) crosses the local DOS minimum in a region of the spectrum formed by the Ti 3d states (the partial DOS is not shown here). However, there is a difference: The peak of the DOS just below  $E_F$  in  $\epsilon$ - $\text{Ti}_2\text{N}$  is located lower in energy than in  $\delta'$ - $\text{Ti}_2\text{N}$ , which indicates that the Ti–Ti bonds in  $\epsilon$ - $\text{Ti}_2\text{N}$  are stronger than in  $\delta'$ - $\text{Ti}_2\text{N}$ , and this may explain the stabilization of the  $\epsilon$  phase instead of the  $\delta'$  phase at low temperatures.

It is well known that  $\delta'$ - $\text{Ti}_2\text{N}$  is derived from the B1 structure by assuming long-range order of the nitrogen vacancies, and by allowing for a shift of the Ti atoms along the fourfold tetragonal axis. A shift of the Ti atoms away from the nitrogen vacancy ( $0.123$  Å) (Ref. 12), as well as towards the vacancy<sup>11</sup> can be found in the literature. A comparison of the computed structures of B1-TiN and  $\delta'$ - $\text{Ti}_2\text{N}$  clearly indicates the shift of the neighbor Ti atoms away from the vacancy by  $0.157$  Å. We also performed additional calculations to establish a possible origin of the tetragonal lattice relaxation in the  $\epsilon$  and  $\delta'$  phases of  $\text{Ti}_2\text{N}$ . For this purpose, we calculated the atomic configuration of the  $\text{Ti}_{32}\text{N}_{31}$  structure that was represented by a 63-atoms cell of B1-TiN<sub>x</sub> with a single nitrogen vacancy in the center. After relaxation, we identified a uniform shift of the Ti atoms around the N vacancy away from this vacancy by  $0.107$  Å, and a shift of the

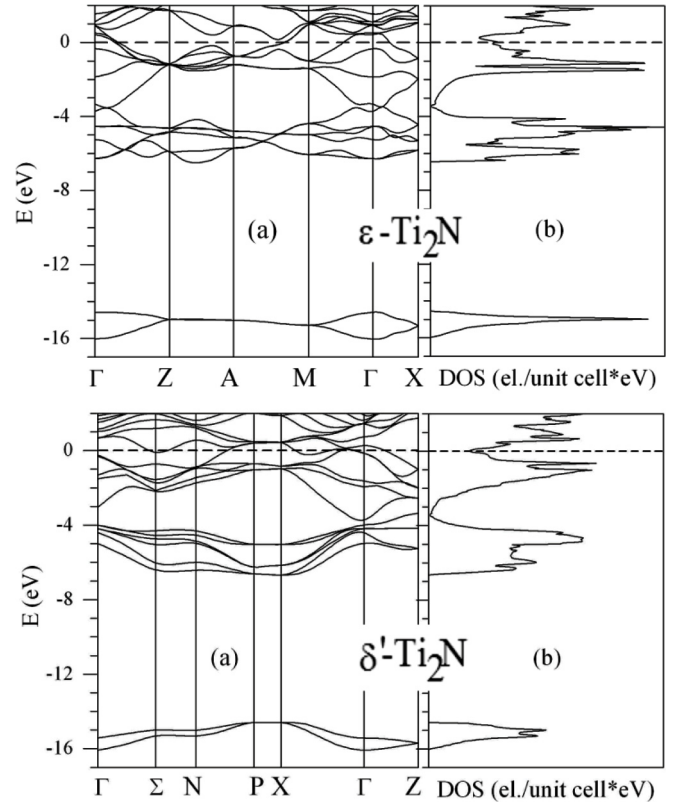


FIG. 2. Band structure in some symmetry directions of the (a) BZ and (b) densities of states (DOS) for  $\epsilon$ - $\text{Ti}_2\text{N}$  and  $\delta'$ - $\text{Ti}_2\text{N}$ . The dashed line locates the Fermi level ( $E_F$ ), taken as zero of energy.

next neighbor atoms towards the vacancy by  $0.015$  Å. Since the uniform lattice relaxation around the vacancy could be related to the periodic boundary conditions (PBC) that were imposed to the cell and to the small size of the unit cell, we calculated a finite cluster  $\text{Ti}_{14}\text{N}_{18}$  without imposing the PBC (see Sec. II). We found an outward shift of the Ti atoms  $\Delta_x = \Delta_y = 0.156$  Å,  $\Delta_z = 0.157$  Å. Although further work may be required, the later results suggest that the tetragonal structure of both the  $\epsilon$  and  $\delta'$  phases of  $\text{Ti}_2\text{N}$  is related to the tetragonal local lattice distortion around the nitrogen vacancy.

Now let us address the following question: Can the  $\delta'$ - $\text{Ti}_2\text{N}$  phase be stable at low temperatures as was found in some experiments? To answer this question, we calculated the phonon dispersion curves along some symmetry directions of the  $\mathbf{k}$  space and the phonon densities of states (PHDOS) for the  $\epsilon$  and  $\delta'$  phases of  $\text{Ti}_2\text{N}$ . The calculated phonon spectrum and the PHDOS of these phases are shown in Fig. 3. We note that the phonon spectrum of the  $\epsilon$  phase does not contain any soft modes, which explains why this phase should be dynamically stable. On the contrary, a softening of the acoustic phonon modes around the X point is observed in the phonon spectrum of  $\delta'$ - $\text{Ti}_2\text{N}$ , which implies that this phase is dynamically unstable. We suppose that the soft phonon frequencies will increase with temperature and, correspondingly, the dynamically unstable  $\delta'$ - $\text{Ti}_2\text{N}$  structure should be stabilized at high temperatures in agreement with experiments.<sup>8–10</sup> A similar situation is observed for other transition metal nitrides with the B1 structure, such as VN and



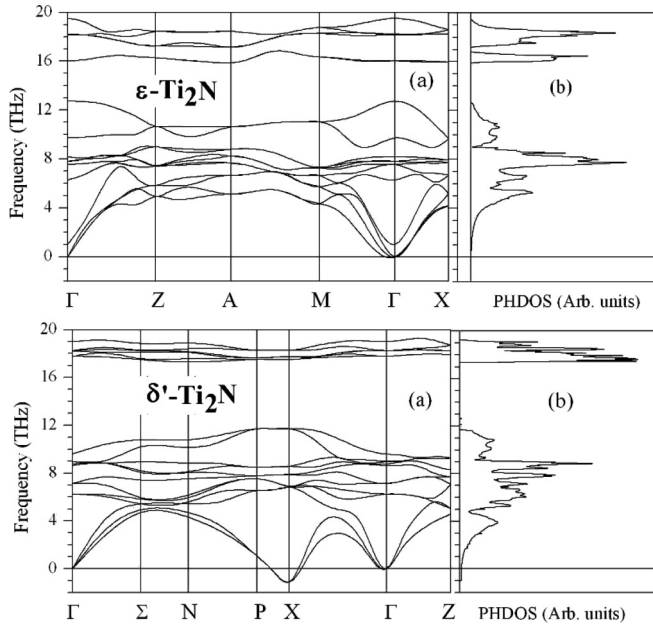


FIG. 3. Phonon dispersion curves along some high symmetry directions of the BZ (a) and phonon density of states (PHDOS) (b) for  $\epsilon$ -Ti<sub>2</sub>N and  $\delta'$ -Ti<sub>2</sub>N.

NbN: these nitrides display soft phonon acoustic modes around the  $X$  point,<sup>24,25</sup> the reason for this being they can crystallize with the stoichiometric  $B1$  structure only at high temperatures, or with a lower atomic composition on the nonmetal sublattice leading to vacancy-stabilized phases.<sup>1,2</sup>

For some TMC, phonon anomalies are caused by a resonance-like increase of the dielectric screening at specific phonon wave vectors. This can be caused by the specific “jungle-gym” topology of the Fermi surface (as in the case of TMC with a valence-electron concentration equal to 9: TiN, ZrN, VC, NbC),<sup>26,27</sup> or by the resonance-like increase of the electron-ion form factors at particular phonon wave vectors  $\mathbf{q}$  (as in the case of the TMC with a valence-electron concentration equal to 10, e.g., VN, NbN, TiO).<sup>28</sup> For the latter compounds, the longitudinal electron-ion form factors drastically increase for  $\mathbf{q} = 2\pi/a$  (0 0 1) ( $X$  point), owing to interband transitions between the  $W$  points.<sup>28</sup> Given these findings, let us return to the discussion of the origin of the phonon anomalies in  $\delta'$ -Ti<sub>2</sub>N. We calculated the Fermi surfaces of several bands for both the  $\epsilon$  and  $\delta'$  phases of Ti<sub>2</sub>N. The computed Fermi surfaces are shown in Fig. 4. For  $\delta'$ -Ti<sub>2</sub>N, a thorough inspection of the Fermi surface topology showed that any nesting regions that could cause a resonance-like increase of the dielectric screening are lacking. It follows that, for  $\delta'$ -Ti<sub>2</sub>N, the soft acoustic modes at the  $X$  point are not a consequence of the specific Fermi surface topology (cf. Fig. 4), but instead are most likely caused by the abnormal dependence of the matrix elements of the electron-phonon interaction at the  $X$  point.

Since we have the information on the phonon spectra of both the  $\epsilon$  and  $\delta'$  phases of Ti<sub>2</sub>N, it would be reasonable to estimate the structural stability of these phases taking into account the vibrational contribution  $F_{\text{vib}}$  to the Helmholtz free energy. We calculated Helmholtz free energy differences  $\Delta F(T) = \Delta E_{\text{tot}} + \Delta F_{\text{vib}}(T)$  between these phases neglecting

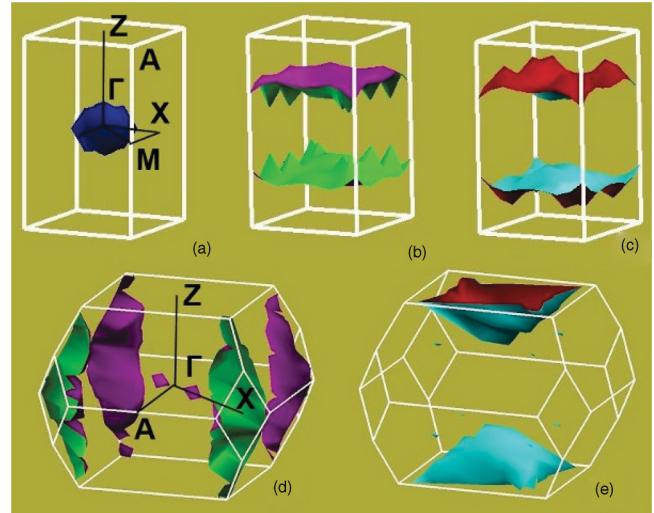


FIG. 4. (Color online) Fermi surface of the (a) 12th band, (b) 13th band, and (c) 14th band for  $\epsilon$ -Ti<sub>2</sub>N and of the (d) 13th band and (e) 14th band for  $\delta'$ -Ti<sub>2</sub>N.

the soft phonon mode contribution to  $F_{\text{vib}}$  in  $\delta'$ -Ti<sub>2</sub>N (the negative frequency region in the PHDOS, cf. Fig. 3). We suppose that such an approach will be quite justified since (i) the integrated PHDOS in this region approximates only to 0.01% of the value of the total integrated PHDOS and (ii) the frequencies of the soft modes will increase with temperature.

Figure 5 shows that the  $\delta'$  phase will be more stable than the  $\epsilon$  phase at temperatures above the critical temperature of 1250 K. The decomposition of the vibrational free energy into the internal energy and the entropy (not shown here) indicates that the transition is driven by the vibrational entropy. Our calculated value of the  $\epsilon$  to  $\delta'$  transition temperature of 1250 K is close to the experimental annealing temperature at which the structural transformation is activated.<sup>5,8–10</sup>

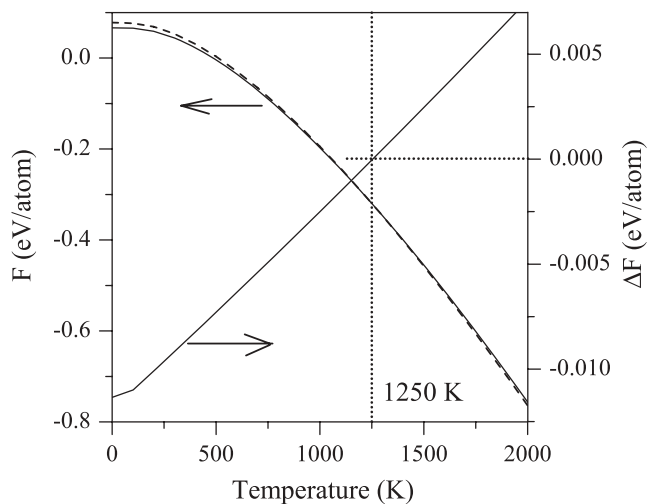


FIG. 5. Free energy for the  $\epsilon$  and  $\delta'$  phases of Ti<sub>2</sub>N ( $F$ ) and free energy difference  $\Delta F = F(\epsilon\text{-Ti}_2\text{N}) - F(\delta'\text{-Ti}_2\text{N})$  as functions of temperature.

### B. Ti<sub>2</sub>N structures under pressure

To predict possible stable phases of Ti<sub>2</sub>N under high pressure we calculated the total energies ( $E_T$ ) of all the Ti<sub>2</sub>N phases presented in Table I as functions of cell volume ( $V$ ). An analysis of the calculated volume dependence of the total energies  $E_T(V)$ ,  $7.8-8.3 < V < 13.6-14.8 \text{ \AA}^3/\text{atom}$ , enabled us to identify the phases that could be derived from  $\epsilon$ -Ti<sub>2</sub>N at high pressure. The total energies of these phases as functions of cell volume obtained by means of the six-order polynomial fit to the data points calculated by the first-principles procedure<sup>16</sup> are shown in Fig. 6. One can see from Fig. 6 that  $\epsilon$ -Ti<sub>2</sub>N will transform into Cd<sub>2</sub>I-type Ti<sub>2</sub>N (space group  $P-3m1$ ), and the second phase will transform into Al<sub>2</sub>Cu-type Ti<sub>2</sub>N (space group  $I4/mcm$ ) with increasing pressure. We should verify whether these new pressure-induced phases are dynamically stable. The phonon dispersion curves for Cd<sub>2</sub>I-type and Al<sub>2</sub>Cu-type Ti<sub>2</sub>N at equilibrium and under pressure are presented in Fig 6. The phonon dispersions clearly indicate that the Al<sub>2</sub>Cu-type Ti<sub>2</sub>N phase is dynamically stable at equilibrium and under pressure, whereas the Cd<sub>2</sub>I-Ti<sub>2</sub>N phase is dynamically unstable at any pressures owing to the availability of the condensed acoustic modes around the A and  $\Gamma$  points.

To determine a new structure that could be derived from the Cd<sub>2</sub>I type Ti<sub>2</sub>N phase by a condensation of the soft modes at the A and  $\Gamma$  points, we performed a symmetry analysis using the ISOTROPY code.<sup>29</sup> The possible structures originated from Cd<sub>2</sub>I-type Ti<sub>2</sub>N are listed in Table II. Given the sequence of the phonon frequencies at the A point:  $2A_{3-} < 2A_{3+} < A_{2-} < A_{1+} < A_{2-} < 2A_{3-}$ , the structures that could be originated from Cd<sub>2</sub>I-type Ti<sub>2</sub>N by means of a condensation of the acoustic  $A_{3-}$  mode should have the following symmetries: No. 12,  $C2/m$ ; No.15,  $C2/c$ ; No. 2,  $P-1$ . At the  $\Gamma$  point, the frequencies are sorted out as follows:  $2\Gamma_{3-} < \Gamma_{2-} < 2\Gamma_{3+} < \Gamma_{1+} < \Gamma_{2-} < 2\Gamma_{3-}$ . This means that a deformation of the unit cell according to the acoustic mode  $\Gamma_{3-}$ , or a shift of the sublattices in accordance with the optical

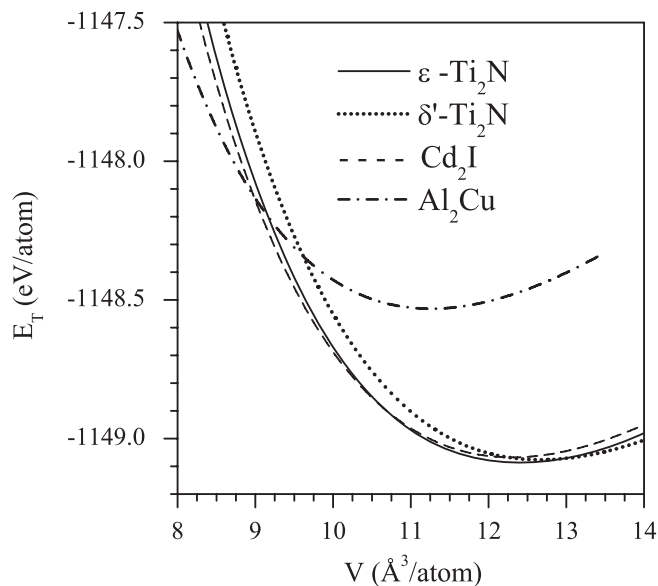


FIG. 6. Total energy ( $E_T$ ) as a function of cell volume ( $V$ ) for various phases of Ti<sub>2</sub>N.

TABLE II. Classification of the possible stable phases along particular directions (order parameter space) (Ref. 29).  $a$  and  $b$  are the amplitudes of the normal coordinate of the corresponding mode that is characterized with a specific irreducible representation (IRREP) at the A and  $\Gamma$  points of Cd<sub>2</sub>I-type Ti<sub>2</sub>N (space group  $P-3m1$ , No. 164).

IRREP (ISOTROPY)	IRREP	No.	Space group	Direction
$A_{1+}$	$A_{1g}$	164	$P-3m1$	$P1(a)$
$A_{2-}$	$A_{2u}$	164	$P-3m1$	$P1(a)$
$A_{3+}$	$E_g$	12	$C2/m$	$P1(a,0)$
		15	$C2/c$	$P2(0,a)$
		2	$P-1$	$C1(a,b)$
$A_{3-}$	$E_u$	12	$C2/m$	$P2(0,a)$
		15	$C2/c$	$P1(a,0)$
$\Gamma_{1+}$	$A_{1g}$	2	$P-1$	$C1(a,b)$
		8	$Cm$	$P1(a,0)$
$\Gamma_{2-}$	$A_{2u}$	5	$C2$	$P2(0,a)$
		1	$P1$	$C1(a,b)$

modes  $\Gamma_{3-}$ ,  $\Gamma_{2-}$ ,  $\Gamma_{3+}$ , and  $\Gamma_{2-}$  should lead to the formation of one of the structures listed in Table II. To find the most stable structure that could be derived from Cd<sub>2</sub>I-type Ti<sub>2</sub>N, one should compare the total energies of the different structures that are listed in Table II. However, this is tedious work and is out of the scope of the present study. Here, we calculated only the Au<sub>2</sub>Te-type Ti<sub>2</sub>N structure (space group  $C2/m$ , No. 12) that is listed in Table II to illustrate the formation of a new phase by means of a condensation of the  $\Gamma_{3+}$  or  $A_{3-}$  modes in Cd<sub>2</sub>I-type Ti<sub>2</sub>N. The phonon spectrum of the Au<sub>2</sub>Te-type Ti<sub>2</sub>N structure at equilibrium is shown in Fig. 7. There are no imaginary

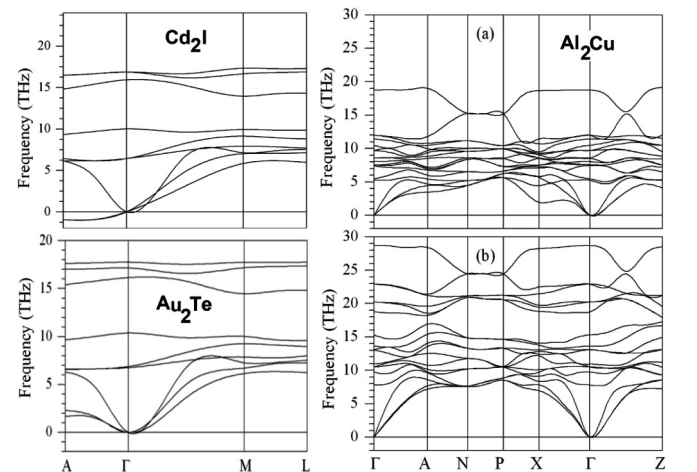


FIG. 7. Phonon dispersion curves along some high symmetry directions of the BZ for Cd<sub>2</sub>I- and Au<sub>2</sub>Te-type Ti<sub>2</sub>N at equilibrium, and for Al<sub>2</sub>Cu-type Ti<sub>2</sub>N at (a) equilibrium and (b) under pressure  $P = 120$  GPa (higher than the transition pressure). The Au<sub>2</sub>Te-type Ti<sub>2</sub>N structure represents a slightly distorted hexagonal version of the Cd<sub>2</sub>I-type Ti<sub>2</sub>N structure; hence the same notation for the symmetry points is used for both structures. “Negative” frequencies actually mean “imaginary” (negative squared frequencies).

TABLE III. Fitting parameters of the Murnaghan equation (Ref. 30):  $V_0$ —unit cell volume,  $E_0$ —total energy,  $B_0$ —bulk modulus,  $B'_0$ —bulk modulus derivative.

Phase	$V_0$ ( $\text{\AA}^3/\text{atom}$ )	$E_0$ (eV/atom)	$B_0$ (GPa)	$B'_0$
$\epsilon$ -Ti <sub>2</sub> N	12.396	0.000	203.8	3.715
Au <sub>2</sub> Te	12.412	0.017	197.7	3.553
Al <sub>2</sub> Cu	11.275	0.555	195.9	3.529

frequencies in the phonon dispersion curves of Au<sub>2</sub>Te-type Ti<sub>2</sub>N at equilibrium and under pressure (not shown here), and therefore this structure should be dynamically stable.

To clarify in more detail the phase transformations in  $\epsilon$ -Ti<sub>2</sub>N under pressure taking into account the finding discussed above, we calculated the enthalpies ( $H$ ) and cell volume ( $V$ ) of  $\epsilon$ -Ti<sub>2</sub>N, Au<sub>2</sub>Te-Ti<sub>2</sub>N, and Al<sub>2</sub>Cu-Ti<sub>2</sub>N. For this purpose, we used the traditional Murnaghan equation of states.<sup>30</sup> There are four fitting parameters in the Murnaghan equation that correspond to an equilibrium state:  $V_0$ —unit cell volume,  $B_0$ —bulk modulus,  $B'_0$ —bulk modulus derivative,  $E_0$ —total energy. These parameters obtained from the Murnaghan fit are included in Table III. In Fig. 8 we show the values of  $H$  and  $V$  as functions of pressure ( $P$ ). Given these results, as well the results of the total energy and phonon spectrum calculations for various phases of Ti<sub>2</sub>N under pressure, we predict the following sequence of phase transformations in  $\epsilon$ -Ti<sub>2</sub>N under pressure:  $\epsilon$ -Ti<sub>2</sub>N (space group  $P4/mmm$ ),  $P = 77.5$  GPa  $\rightarrow$  Au<sub>2</sub>Te-type (space group  $C2/m$ ),  $P = 86.7$  GPa  $\rightarrow$  Al<sub>2</sub>Cu-type (space

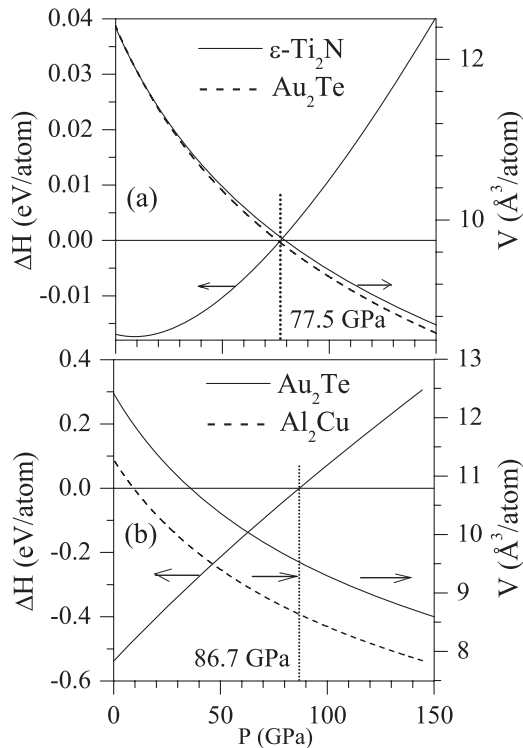


FIG. 8. Difference of enthalpies (a)  $\Delta H = H(\epsilon\text{-Ti}_2\text{N}) - H(\text{Au}_2\text{Te-type Ti}_2\text{N})$  and (b)  $\Delta H = H(\text{Au}_2\text{Te-type Ti}_2\text{N}) - H(\text{Al}_2\text{Cu-type Ti}_2\text{N})$  and cell volume ( $V$ ) for various phases of Ti<sub>2</sub>N as functions of pressure ( $P$ ).

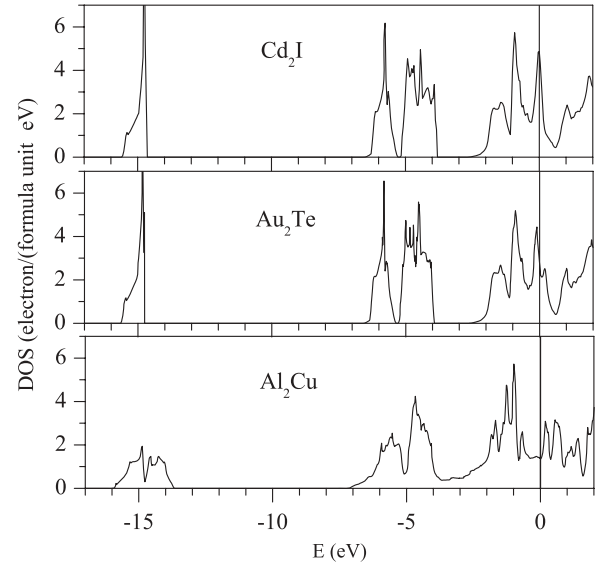


FIG. 9. Density of states (DOS) of the Cd<sub>2</sub>I-, Au<sub>2</sub>Te-, and Al<sub>2</sub>Cu-type phases of Ti<sub>2</sub>N at equilibrium. The vertical line locates the Fermi level ( $E_F$ ), taken as zero of energy.

group  $I4/mcm$ ). All these phase transformations are first order in nature since the cell volumes change abruptly at the transition points. We note that the transition pressure obtained from the six-order polynomial fit was 79.7 and 86.2 GPa for the first and second transformations, respectively. The small differences in the transition pressures are supposed to be likely due to the different ranges of cell volumes considered in the two procedures.

Let us investigate the electronic structure of these new pressure-induced phases. The densities of states of the Cd<sub>2</sub>I-, Au<sub>2</sub>Te- and Al<sub>2</sub>Cu-type Ti<sub>2</sub>N phases at equilibrium are shown in Fig. 9. Below, we will attempt to estimate phase stability following the simple rule: The lower the density of states is at the Fermi level, the more stable is the structure. The motivation of this is that the high DOS at the Fermi level causes the existence of soft phonon modes in the long-wave region, and their collapse leads to a structural transformation. Figures 2 and 9 show that the Fermi level for all the computed structures of Ti<sub>2</sub>N is located in a local minimum of the DOS except for Cd<sub>2</sub>I-type Ti<sub>2</sub>N, where a high DOS is associated with the Fermi level. Thus, the high DOS at the Fermi level in Cd<sub>2</sub>I-type Ti<sub>2</sub>N can be one of the reasons of the dynamical instability of this phase. It is seen that the small lattice distortion in Cd<sub>2</sub>I-type Ti<sub>2</sub>N resulting in the formation of the Au<sub>2</sub>Te-type phase of Ti<sub>2</sub>N, in turn, leads to a splitting of the peak of the DOS near the Fermi level.

#### IV. CONCLUSION

First-principles calculations of the electronic and phonon structures were performed and, on their basis, the phase stability of various phases of Ti<sub>2</sub>N at equilibrium and under pressure was examined. The analysis of the dependencies of enthalpy and phonon spectra on the pressure of these Ti<sub>2</sub>N phases enabled us to bring the following conclusions.  $\epsilon$ -Ti<sub>2</sub>N at zero pressure is the most stable phase in agreement with the experiment and previous total-energy calculations. The

$\delta'$ -Ti<sub>2</sub>N phase can only exist at high temperature due to the availability of soft acoustic modes at the *X* point. We supposed that the tetragonal structure of both the  $\epsilon$  and  $\delta'$  phases of Ti<sub>2</sub>N is caused by a tetragonal local-lattice distortion around the N vacancy. The following phase transformations in  $\epsilon$ -Ti<sub>2</sub>N under pressure at zero temperature are predicted:  $\epsilon$ -Ti<sub>2</sub>N (space group *P4/mmm*),  $P = 77.5$  GPa  $\rightarrow$  Au<sub>2</sub>Te-type (space group *P-3m1*),  $P = 86.7$  GPa  $\rightarrow$  Al<sub>2</sub>Cu-type (space group *I4/mcm*).

## ACKNOWLEDGMENTS

This work was supported by the STCU Contract No. 5539. The work of P.T. was performed under the auspices of the US Department of Energy by the Lawrence Livermore National Laboratory under Contract No. DE-AC52-07NA27344. We thank R. Eibler for providing the information on the band-structure calculations of Ti<sub>2</sub>N.

- 
- <sup>1</sup>L. E. Tot, *Transition Metal Carbides and Nitrides* (Academic, New York, 1971).
- <sup>2</sup>A. I. Gusev and A. A. Rempel, *Phys. Status Solidi A* **163**, 273 (1997).
- <sup>3</sup>S. Veprek and S. Reiprich, *Thin Solid Films* **268**, 64 (1995).
- <sup>4</sup>C. H. de Novion and J. P. Landesman, *Pure Appl. Chem.* **57**, 1391 (1985).
- <sup>5</sup>A. Alamo and C. H. de Novion, 7<sup>th</sup> International Conference on Solid Compounds of Transition Elements, Grenoble, June, 1982, P. II-A-1.
- <sup>6</sup>B. Holmberg, *Acta Chem. Scand.* **16**, 1255 (1962).
- <sup>7</sup>I. Khidirov, *Russian J. Inorganic Chemistry* **56**, 298 (2011).
- <sup>8</sup>W. Lengauer and P. Ettmayer, *High Temp. High Press.* **19**, 673 (1987).
- <sup>9</sup>W. Lengauer and P. Ettmayer, *High Temp. High Press.* **22**, 13 (1990).
- <sup>10</sup>E. Etchessahar, Y.-U. Sohn, M. Harmelin, and J. Debuigne, *J. Less-Common Met.* **167**, 261 (1991).
- <sup>11</sup>S. Nakagura and T. Kusunoki, *J. Appl. Cryst.* **10**, 52 (1977).
- <sup>12</sup>A. N. Christensen, A. Alamo, and J. P. Landesman, *Acta. Cryst. C* **41**, 1009 (1985).
- <sup>13</sup>W. Lengauer, *Acta Metall. Mater.* **39**, 2985 (1991).
- <sup>14</sup>R. Eibler, *J. Phys.: Condens. Matter* **5**, 5261 (1993).
- <sup>15</sup>R. Eibler, *J. Phys.: Condens. Matter* **19**, 196226 (2007).
- <sup>16</sup>S. Baroni, A. Dal Corso, S. de Gironcoli, P. Giannozzi, C. Cavazzoni, G. Ballabio, S. Scandolo, G. Chiarotti, P. Focher, A. Pasquarello, K. Laasonen, A. Trave, R. Car, N. Marzari, and A. Kokalj, <http://www.pwscf.org>.
- <sup>17</sup>D. Vanderbilt, *Phys. Rev. B* **41**, 7892 (1990).
- <sup>18</sup>J. P. Perdew, K. Burke, and M. Ernzerhof, *Phys. Rev. Lett.* **77**, 3865 (1996).
- <sup>19</sup>H. J. Monkhorst and J. D. Pack, *Phys. Rev. B* **13**, 5188 (1976).
- <sup>20</sup>S. R. Billeter, A. Curioni, and W. Andreoni, *Comput. Mater. Sci.* **27**, 437 (2003).
- <sup>21</sup>S. Baroni, S. De Gironcoli, A. Dal Corso, and P. Giannozzi, *Rev. Mod. Phys.* **73**, 515 (2001).
- <sup>22</sup>S.-Q. Wang and L. H. Allen, *J. Appl. Phys.* **79**, 2446 (1996).
- <sup>23</sup>*Handbook of Chemistry and Physics*, edited by R. C. Weast, M. J. Astle, and W. H. Beyer, (Chemical Rubber Co., Boca Raton, FL, 1988), Vol. 69.
- <sup>24</sup>V. I. Ivashchenko, P. E. A. Turchi, and E. I. Olifan, *Phys. Rev. B* **82**, 054109 (2010).
- <sup>25</sup>E. I. Isaev, S. I. Simak, I. A. Abrikosov, R. Ahuja, Yu. Kh. Vekilov, M. I. Katsnelson, A. I. Lichtenstein, and B. Johansson, *J. Appl. Phys.* **101**, 123519 (2007).
- <sup>26</sup>M. Gupta and A. J. Freeman, *Phys. Rev. Lett.* **37**, 364 (1976).
- <sup>27</sup>B. M. Klein, D. A. Papaconstantopoulos, and L. L. Boyer, *Solid State Commun.* **20**, 937 (1976).
- <sup>28</sup>W. Weber, P. Roedhammer, L. Pintschovius, W. Reichardt, F. Gompf, and A. N. Christensen, *Phys. Rev. Lett.* **43**, 868 (1979).
- <sup>29</sup>H. T. Stokes, D. M. Hatch, and B. J. Campbell, ISOTROPY, <http://stokes.byu.edu/isotropy.html> (2007).
- <sup>30</sup>F. D. Murnaghan, *Proc. Natl. Acad. Sci. USA* **30**, 244 (1944).